Received: 6 May 2019 | Accepted: 25 June 2019

DOI: 10.1002/pamm.201900100

# A concept for aortic dissection with fluid-structure-crack interaction

**Richard Schussnig**[1,2,*] and **Thomas-Peter Fries**[1,2]

[1] Institute of Structural Analysis, Graz University of Technology, Graz, Austria
[2] Graz Center of Computational Engineering, Graz University of Technology, Graz, Austria

In aortic dissection, the layers composing the aorta rupture, allowing blood to enter the vessel wall. This process is modeled applying a monolithic fluid-structure interaction framework, formulating the Navier-Stokes equations for incompressible flows as well as the mixed finite strain elastodynamics equations in the Lagrangian frame of reference. Continuous test- and trial function spaces are employed in the whole domain, rendering the coupling straightforward. Within this contribution, a predefined function indicating failure is used to convert solid to fluid elements, thereby mimicing tissue rupture.



## 1 Introduction

Substantial advances in the computational modeling of the cardiovascular system and its pathologies were made during the past decades. Both, chronic and acute aortic dissection are highly dangerous health conditions, requiring medication, monitoring or immediate surgical treatment. It is expected that a proper modeling and simulation of aortic dissection may significantly help to understand the sequence of events ultimately leading to false lumen propagation and/or complete rupture of the aorta. Thus, the long-term aim of the present study is to develop a computational model, able to resolve the process of coupled tissue rupture and fluid-flow, in order to lay the foundation for substantial diagnostic tools used for clinical support.
The so-called false lumen propagation, being the ongoing separation or rupture of layers composing the aorta, allows for blood entering the vessel wall, thereby enlarging the fluid flow domain. Vice versa, the tissue displacement governs the deformation of the fluid domain. Across this moving and evolving interface, i.e., at the joint boundary of fluid and solid sub-domains, continuity of tractions, velocities and displacements holds. Consequently, modeling this process necessitates the formulation of a strongly coupled fluid-structure interaction problem in a biomedical setting.

## 2 Governing Equations

Within this contribution, the haemodynamics are represented by the instationary Navier-Stokes equations for incompressible flows. In the arbitrary Lagrangian–Eulerian framework, a continuous, bijective mapping $\hat{\mathcal{A}}_t$ from the joint reference domain $\hat{\Omega} := \hat{\Omega}_f \cup \hat{\Omega}_s$ to the current domain $\Omega(t)$ is introduced for $t \in \mathcal{I}_t := (0, T]$, with $T > 0$ being the end time

$$\hat{\mathcal{A}}_t : \hat{\Omega} \times \mathcal{I}_t \to \Omega(t)\,, \quad \hat{\mathcal{A}}_t(t, \hat{x}) := \hat{\boldsymbol{x}} + \hat{\boldsymbol{u}}(t, \hat{\boldsymbol{x}}) \tag{1}$$

and $\hat{\boldsymbol{u}}$ being the displacement from the reference domain. Additionally defining the displacement gradient $\hat{\mathbf{F}} := \mathbf{I} + \hat{\nabla}\hat{\boldsymbol{u}}$ and the determinant $\hat{J} := \det(\hat{\mathbf{F}})$ the system governing velocity $\hat{\boldsymbol{v}}$ and pressure $\hat{p}$ of the flow is, following [1],

$$\left\{ \begin{array}{rcl} \hat{J}\hat{\rho}_f(\partial_t\hat{\boldsymbol{v}} + [\hat{\mathbf{F}}^{-1}(\hat{\boldsymbol{v}} - \partial_t\hat{\boldsymbol{u}})\cdot\hat{\nabla}]\hat{\boldsymbol{v}} - \hat{\boldsymbol{f}}_f) - \hat{\nabla}\cdot(\hat{J}\hat{\sigma}_f\hat{\mathbf{F}}^{-\top}) &=& \mathbf{0} \\ \hat{\nabla}\cdot(\hat{J}\hat{\mathbf{F}}^{-1}\hat{\mathbf{v}}) &=& \mathbf{0} \quad \text{in } \hat{\Omega}_f \times \mathcal{I}_t \end{array} \right. \tag{2}$$

with the transformed fluid Cauchy stress tensor $\hat{\sigma}_f := -\hat{p}_f\mathbf{I} + \hat{\rho}_f\hat{\nu}_f(\hat{\nabla}\hat{\boldsymbol{v}}\hat{\mathbf{F}}^{-1} + \hat{\mathbf{F}}^{-\top}(\hat{\nabla}\hat{\boldsymbol{v}})^{\top})$, the kinematic viscosity $\hat{\nu}_f$ and density $\hat{\rho}_f$ of the fluid and a load per unit volume $\hat{\boldsymbol{f}}_f$, transformed from the current domain. The arterial wall is modeled as a hyperelastic solid [2], governed by the geometrically nonlinear elastodynamics equations in mixed form, denoting by $\hat{\boldsymbol{v}}$ and $\hat{\boldsymbol{u}}$ the velocity and displacement of the solid respectively

$$\hat{\rho}_s(\partial_t\hat{\boldsymbol{v}} - \hat{\boldsymbol{f}}_s) - \hat{\nabla}\cdot(\hat{\mathbf{F}}\hat{\boldsymbol{\Sigma}}_s) = \mathbf{0} \quad \text{in } \hat{\Omega}_s \times \mathcal{I}_t \quad \text{with } \hat{\boldsymbol{\Sigma}}_s := 2\mu_s\hat{\mathbf{E}} + \lambda_s tr(\hat{\mathbf{E}})\mathbf{I}\ , \ \ \hat{\mathbf{E}} := 0.5(\hat{\mathbf{F}}^{\top}\hat{\mathbf{F}} - \mathbf{I}) \tag{3}$$

with Lamé coefficients $\mu_s = E_s/(2(1+\nu_s))$ and $\lambda_s = 2\nu_s\mu_s/(1-2\nu_s)$, Young's modulus $E_s$ and Poisson ratio $\nu_s$, second Piola-Kirchhoff stress tensor $\hat{\boldsymbol{\Sigma}}_s$, Green-Lagrange strain tensor $\hat{\mathbf{E}}$ and force per unit volume $\hat{\boldsymbol{f}}_s$, defined in the reference domain. The fluid-structure interface's displacement is extended into the fluid reference domain utilizing a harmonic mesh motion model with stiffening [3]

$$-\hat{\nabla}\cdot(\hat{\alpha}_u\hat{J}^{-1}\hat{\nabla}\hat{\boldsymbol{u}}) = \mathbf{0} \quad \text{in } \hat{\Omega}_f \quad \text{with } \hat{\alpha}_u > 0. \tag{4}$$

* Corresponding author: e-mail schussnig@tugraz.at

Equations (2), (3) and (4) are naturally equipped with proper initial conditions, boundary- and coupling conditions, which are omitted for the sake of brevity. Within this preliminary work, tissue failure is completely prescribed by an indicating function of space and time. Restricting tissue failure to certain regions may be a physiologically valid assumption in the application at hand, but crack front position must be considered an unknown in future studies.

## 3 Discretisation

Defining the vector-valued Hilbert spaces $\hat{\mathcal{V}}_D^v$ and $\hat{\mathcal{V}}_D^u$ on $\hat{\Omega} \subset \mathbb{R}^d$, incorporating the Dirichlet boundary conditions for velocities and displacements respectively, the variational formulation of the fluid-structure interaction problem is:
Find $\{\hat{\boldsymbol{v}}, \hat{\boldsymbol{u}}, \hat{p}\} \in \{\hat{\mathcal{V}}_D^v\} \times \{\hat{\mathcal{V}}_D^u\} \times \{\mathcal{L}^2(\hat{\Omega})\}$, such that $\hat{\boldsymbol{v}}(0, \hat{\boldsymbol{x}}) = \bar{\boldsymbol{v}}_0$, $\hat{\boldsymbol{u}}(0, \hat{\boldsymbol{x}}) = \bar{\boldsymbol{u}}_0$ and for almost all $t \in \mathcal{I}_t$ it holds

$$
\begin{aligned}
(\hat{J}\hat{\rho}_f \partial_t \hat{\boldsymbol{v}}, \hat{\boldsymbol{\psi}}^v)_{\hat{\Omega}_f} + (\hat{\rho}_f \hat{J}([\hat{\mathbf{F}}^{-1}(\hat{\boldsymbol{v}} - \partial_t \hat{\boldsymbol{u}}) \cdot \hat{\nabla}]\hat{\boldsymbol{v}} - \hat{\boldsymbol{f}}_f), \hat{\boldsymbol{\psi}}^v)_{\hat{\Omega}_f} + (\hat{J}\hat{\sigma}_f \hat{\mathbf{F}}^{-\top}, \hat{\nabla}\hat{\boldsymbol{\psi}}^v)_{\hat{\Omega}_f} & \\
+(\hat{\rho}_s(\partial_t \hat{\boldsymbol{v}} - \hat{\boldsymbol{f}}_s), \hat{\boldsymbol{\psi}}^v)_{\hat{\Omega}_s} + (\hat{\mathbf{F}}\hat{\boldsymbol{\Sigma}}_s, \hat{\nabla}\hat{\boldsymbol{\psi}}^v)_{\hat{\Omega}_s} - \langle \hat{\rho}_f \hat{\nu}_f \hat{J}(\hat{\mathbf{F}}^{-\top}\hat{\nabla}\hat{\boldsymbol{v}})\hat{\mathbf{F}}^{-\top}\hat{\boldsymbol{n}}_f, \hat{\boldsymbol{\psi}}^v \rangle_{\hat{\Gamma}_{out}} &= \mathbf{0} \quad \forall \hat{\boldsymbol{\psi}}^v \in [\mathcal{H}_0^1(\hat{\Omega})]^d \\
(\partial_t \hat{\boldsymbol{u}} - \hat{\boldsymbol{v}}, \hat{\boldsymbol{\psi}}^u)_{\hat{\Omega}_s} + (\hat{\alpha}_u \hat{J}^{-1}\hat{\nabla}\hat{\boldsymbol{u}}, \hat{\nabla}\hat{\boldsymbol{\psi}}^u)_{\hat{\Omega}_f} &= \mathbf{0} \quad \forall \hat{\boldsymbol{\psi}}^u \in [\mathcal{H}_0^1(\hat{\Omega})]^d \\
(\hat{\nabla} \cdot (\hat{J}\hat{\mathbf{F}}^{-1}\hat{\boldsymbol{v}}), \hat{\boldsymbol{\psi}}^p)_{\hat{\Omega}_f} &= 0 \quad \forall \hat{\boldsymbol{\psi}}^p \in \mathcal{L}^2(\hat{\Omega}).
\end{aligned}
\tag{5}
$$

In (5), the boundary term $\langle \cdot \rangle_{\hat{\Gamma}_{out}}$ enforces the do-nothing boundary condition on the fluid outflow boundary $\hat{\Gamma}_{out} \subset \partial\hat{\Omega}_f$. Moreover, spurious feedback of the mesh motion equation (4) on the balance of linear momentum is inhibited via choosing $\hat{\alpha}_u \ll 1$. Following [4], the variational formulation (5) is discretized in time using a shifted version of the second order accurate Crank-Nicholson scheme and linearized using the Newton-Raphson method combined with a line-search technique to provide robust and rapid convergence. Spatial discretization of test and trial function spaces $\mathcal{X}_h \subset \mathcal{X}$ is carried out using inf-sup stable Finite Element pairs $Q_k^c / P_{k-1}^{dc}$ for the fluid velocity and pressure and equal order interpolation for velocities and displacements in the entire domain.

## 4 Numerical example

The problem setup, depicted in Fig. 1, consists of a flow in a two-dimensional channel with a length of 5 cm and a width of 2.5 cm. The walls are 3 mm thick, the upper one featuring a 0.1 mm thin layer, whose solid elements are converted to fluid elements, whenever $\varphi := \hat{x} - 0.025 - 0.0045\,t \leq 0$ in the center of each element, leaving a 0.1 mm thin layer of solid. The parameters in (5) are chosen as $\hat{\rho}_f = 1$ g/cm$^3$, $\hat{\nu}_f = 3.5 \cdot 10^{-6}$ m/s$^2$, $\hat{\rho}_s = 1.2$ g/cm$^3$, $\nu_s = 0.48$, $E_s = 4 \cdot 10^5$ N/m$^2$, $\hat{\boldsymbol{f}}_f = \hat{\boldsymbol{f}}_s = \mathbf{0}$ N/m$^3$ and $\hat{\alpha}_u = 1 \cdot 10^{-8}$. Initial conditions are $\bar{\boldsymbol{v}}_0 = \bar{\boldsymbol{u}}_0 = \mathbf{0}$, the channel walls are fixed at the in- and outlet and feature homogeneous Neumann boundary conditions on the top and bottom boundaries. The flow is driven by the velocity profile $\hat{\boldsymbol{v}} = (\hat{v}_1, 0)^\top$, $\hat{v}_1 \approx -11072.66\hat{x}_2 + 348.79\hat{x}_2 - 0.95$ prescribed at $\hat{x}_1 = 0$ m and the do-nothing boundary condition at $\hat{x}_1 = 0.025$ m. The computations are performed using a timestep size of $\Delta t = 1 \cdot 10^{-3}$ s in an extension of the implementation [4] within the deal.II package [5]. As can be seen in Fig. 2, the mapping $\hat{\mathcal{A}}_t$ remains regular even under strong deformation, highlighting the robustness of the presented approach with respect to collapse of the narrow fluid-filled gap.

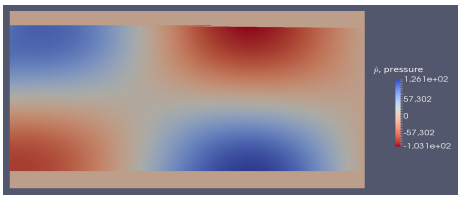


**Fig. 1:** Pressure $\hat{p}$, in $\hat{\Omega}$ at $t = 0.7$ s.

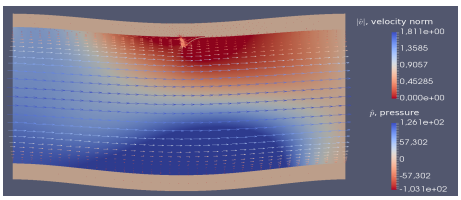


**Fig. 2:** Pressure $\hat{p}$ and velocity $\hat{v}$ in $\Omega(0.9)$.

**Acknowledgements** The authors gratefully acknowledge Graz University of Technology for the financial support of the Lead-project *Mechanics, Modeling and Simulation of Aortic Dissection*.

## References

[1] T. Richter, and T. Wick, Comput Methods Appl Mech Eng **199**, 2633-2642 (2010).
[2] U. Küttler, M. Gee, C. Förster, A. Comerford, and W. Wall, Int J Numer Method Biomed Eng **26**, 305-321 (2010).
[3] T. Wick, Comput Struct, **89**, 1456-1467 (2011).
[4] T. Wick, Arch Num Soft, **1**, 1-19 (2011).
[5] G. Alzetta, D. Arndt, W. Bangerth, V. Boddu, B. Brands, D. Davydov, R. Gassmoeller, T. Heister, L. Heltai, K. Kormann, M. Kronbichler, M. Maier, J.-P. Pelteret, B. Turcksin, and D. Wells, J Num Math, **26**, 173-183 (2018).

 